

RF SYSTEMS OF J-PARC PROTON SYNCHROTRONS FOR HIGH-INTENSITY LONGITUDINAL BEAM OPTIMIZATION AND HANDLING

Fumihiko Tamura*, Masanobu Yamamoto, Masahito Yoshii, Chihiro Ohmori, Yasuyuki Sugiyama,
 Hidefumi Okita, Kiyomi Seiya, Masahiro Nomura, Taihei Shimada, Katsushi Hasegawa,
 Keigo Hara, Ryoosuke Miyakoshi
 J-PARC Center, JAEA & KEK, Tokai-mura, Japan

Abstract

The application of magnetic alloy (MA) cores to the accelerating rf cavities in high intensity proton synchrotrons was pioneered for the J-PARC synchrotrons, the RCS and MR. The MA loaded cavities can generate high accelerating voltages. The wideband frequency response of the MA cavity enables the frequency sweep to follow the velocity change of protons without the tuning loop. The dual harmonic operation, where a single cavity is driven by the superposition of the fundamental and second harmonic rf voltages, is indispensable for the longitudinal bunch shaping to alleviate the space charge effects in the RCS. These advantages of the MA cavity are also disadvantages when looking at them from a different perspective. Since the wake voltage consists of several harmonics, which can cause bucket distortion or coupled-bunch instabilities, the beam loading compensation must be multiharmonic. The operation of tubes in the final stage amplifier is not trivial when accelerating very high intensity beams; the output current is high and the anode voltages also multiharmonic. We summarize our effort against these issues in the operation of the RCS and MR for more than 10 years.

INTRODUCTION

The Japan Proton Accelerator Research Complex (J-PARC) [1] is a high intensity proton facility, which consists of the 400 MeV linac, the 3 GeV Rapid Cycling Synchrotron (RCS) [2], and the 30 GeV Main Ring (MR) [3]. The high intensity output beams from the RCS and MR are used for generation of secondary particles at the Materials and Life Science Experimental Facility (MLF), the Hadron Hall, and the Neutrino Experimental Facility. The main parameters and their rf systems of the RCS and MR are listed in Table 1 and 2, respectively.

The application of magnetic alloy (MA) cores to the accelerating rf cavities in high intensity proton synchrotrons was pioneered for the J-PARC synchrotrons, the RCS and MR. The MA cavities can generate high accelerating voltage required for acceleration of high intensity proton beams. As shown in the tables, the maximum voltage of 440 kV is generated by twelve rf cavities in the RCS and 480 kV is generated by nine cavities in the MR. The MA cavity has wideband frequency response. The Q values of the cavities are set to 2 and 22 by an external inductor [4] and cut-core scheme

Table 1: Parameters of the J-PARC RCS and its RF System

Parameter	Value
Circumference	348.333 m
Energy	0.400–3 GeV
Beam intensity	8.3×10^{13} ppp
Output beam power	1 MW
Accelerating frequency	1.227–1.671 MHz
Harmonic number	2
Maximum rf voltage	440 kV
Repetition rate	25 Hz
No. of cavities	12
Q-value of rf cavity	2

Table 2: Parameters of the J-PARC MR and its RF System

Parameter	Value
Circumference	1567.5 m
Energy	3 – 30 GeV
Beam intensity	2.5×10^{14} ppp
Output beam power	(design) 750 kW
Accelerating frequency	1.67–1.72 MHz
Harmonic number	9
Maximum rf voltage	480 kV
Repetition period	1.16 – 5.2 s
No. of cavities (Fund. + 2nd)	9+2
Q-value of Fund. rf cavity	22

for the RCS and MR, respectively. In both of the RCS and MR, the wideband responses enable the frequency sweep to follow the velocity change of the protons without tuning loops. The MR cavity is driven by the single harmonic rf. The Q value of the RCS cavity is set so that the dual harmonic operation [5], where a single cavity is driven by the superposition of the fundamental and the second harmonic rf voltages, is possible. The dual harmonic operation is indispensable for the longitudinal bunch shaping to alleviate the space charge effects in the beginning of acceleration in the RCS [6, 7].

On the other hand, the wideband frequency response has drawbacks. The wake voltage in the MA cavity is multiharmonic. In the case of the RCS cavity, the wake voltage consists of several higher harmonics. The rf bucket distort-

* fumihiko.tamura@j-parc.jp

Content from this work may be used under the terms of the CC-BY-4.0 licence (© 2023). Any distribution of this work must maintain attribution to the author(s), title of the work, publisher, and DOI

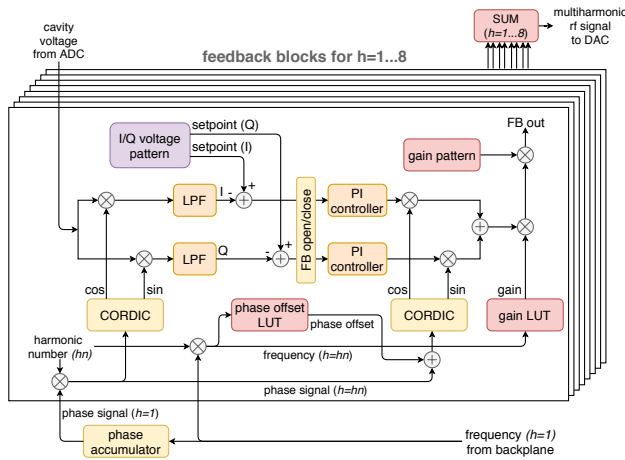


Figure 1: Simplified block diagram of the multiharmonic vector rf voltage control feedback.

tion affects the bunch shape and stability. The MR cavity has a narrower bandwidth compared to that of the RCS, however, it is still wide enough that the wake voltage contains the neighbor harmonics that can contribute to the coupled bunch instabilities.

The output current of the final stage tetrode amplifier is distorted and therefore contains higher harmonics. The tetrode tube operation is not trivial with the wideband RCS cavity. The tube operating condition is a limiting factor of the maximum beam intensity.

In this article, we present our efforts against these issues in the operation of the RCS and MR, for both of the low level rf (LLRF) control and high power rf systems.

MULTIHARMONIC VECTOR RF VOLTAGE CONTROL FEEDBACK

Overview and System Configuration

The original LLRF control system of the RCS and MR was developed during the construction period of the J-PARC. It was configured as a fully digital control system based on the VME platform. The RCS system featured the dual harmonic auto voltage control [5,6] and the multiharmonic feedforward beam loading compensation [8,9]. The MR LLRF control system is similar to the RCS system except that the cavity is driven by a single harmonic, and the multiharmonic feedforward is also employed [10].

The systems worked fairly well for more than ten years, however, it became difficult to maintain the original systems due to the obsolescence of the key FPGAs in the original systems. We decided to develop the new LLRF control systems [11] based on the MTCA.4 (Micro Telecom Computing Architecture [12]). The replacements of the RCS and MR LLRF control systems were done in 2019 and 2022, respectively.

The most significant change in the new system is employment of the I/Q vector voltage feedback for the regulation of the cavity voltage and the beam loading compensation [13].

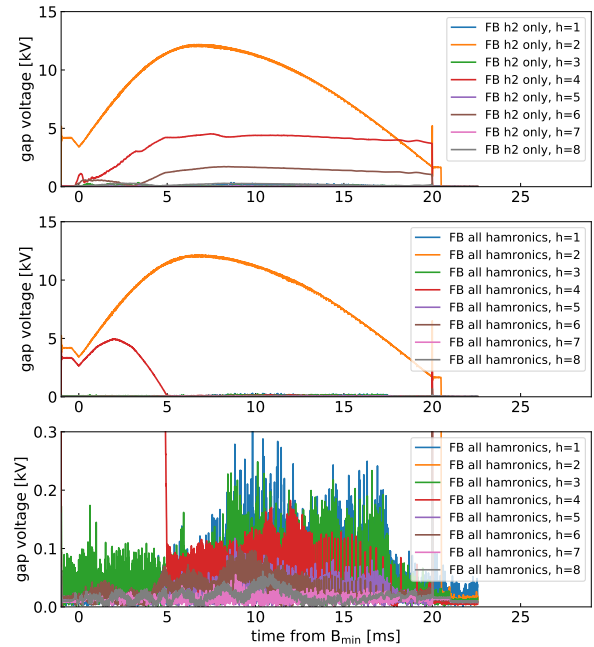


Figure 2: Harmonic components of the gap voltage with acceleration of 1 MW equivalent beam in the cases of (top) that the feedback for the fundamental acceleration harmonic ($h = 2$) is closed and the output of the others are turned off, (middle) the feedbacks for all harmonics are closed, and (bottom) vertically magnified view of the middle plot.

Our commissioning method [8, 10] of the feedforward relies on the linearity of the system. For the very high intensity beams, degradation the performance of the compensation was observed due to the nonlinearity of the tetrode amplifier. Furthermore, the voltage waveform distortion due to the distortion of the amplifier output current becomes intolerable under heavy beam loading that requires high tetrode output current for compensation.

As described above, the voltage regulation and beam loading compensation must be multiharmonic. The simplified block diagram of multiharmonic vector rf voltage control feedback for the RCS is shown in Fig. 1. It consists of eight classical I/Q feedback blocks to control eight harmonics ($h = 1 \dots 8$). The key functions for following the frequency sweep are the phase offset LUT (look-up table) and the gain LUT. To cover very wide frequency from ~ 600 kHz ($h = 1$ minimum) to 6.8 MHz ($h = 8$ maximum), the LUTs keep the feedback conditions of the gain and phase as constant as possible. Also the low pass filter (LPF) has important role to define the feedback characteristics. For the complete details of the LPF design and LUT commissioning, please refer the previous article [13].

RCS Beam Commissioning Results

Prior to the full installation of the new system, the single cavity test was performed. Figure 2 shows the harmonic components of the gap voltage with acceleration of 1 MW

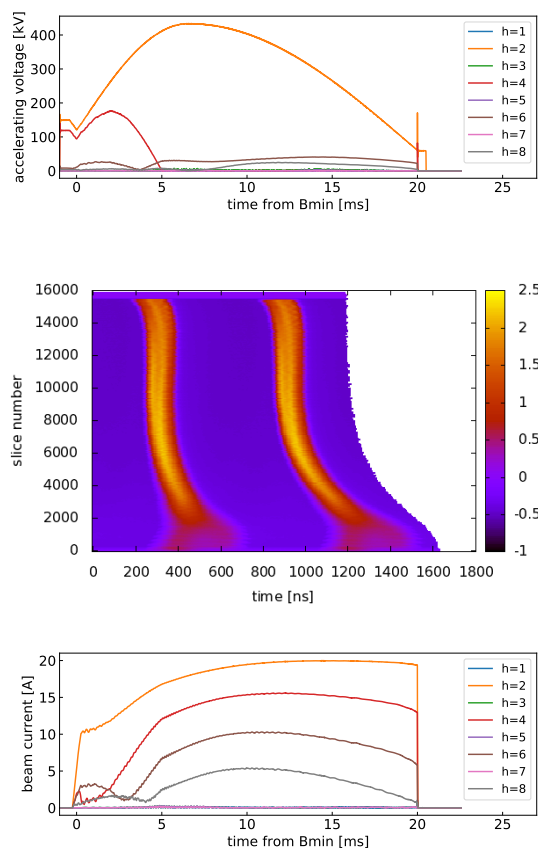


Figure 3: (Top) Harmonic components of the cavity voltage vectorsum, (middle) mountain plot of WCM beam signal, and (bottom) harmonic components of the WCM beam signal, with acceleration of 1 MW equivalent beam.

equivalent beam. In the top plot, the feedback for the fundamental acceleration harmonic ($h = 2$) is closed and the output of the others are turned off. The fundamental harmonic ($h = 2$) is well regulated as the program with the maximum voltage of 12.2 kV. Because of acceleration of two bunches, the wake voltage consists of only even harmonics. The significant components are ($h = 4$) and ($h = 6$), with maximum voltages of 4.6 kV and 1.7 kV, respectively. The ($h = 8$) component is observed but small. The harmonic components with all feedbacks closed are shown in the middle plot, and the vertically magnified view is shown in the bottom plot. The driving harmonics ($h = 2, 4$) are regulated as programmed. After 5 ms, the programmed voltage is zero for ($h = 4$) and it is suppressed less than 0.2 kV. All other harmonics are kept less than 0.3 kV throughout the accelerating period.

Thus, it is proved that the multiharmonic vector rf voltage control feedback can regulate eight harmonics at design beam power of 1 MW. The multiharmonic beam loading in the MA cavity is successfully compensated, as well as the voltage distortion due to the distorted output current of the tetrode amplifier.

After the full replacement of the LLRF control system in 2019, the feedback commissioning was performed [14].

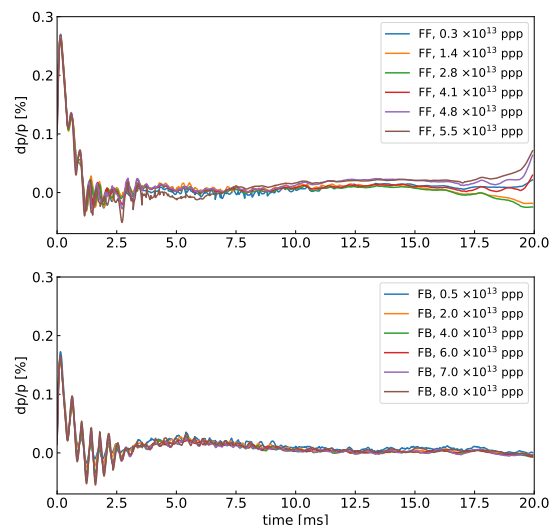


Figure 4: Momentum deviations (dp/p) of the beams with various intensities from injection to extraction, (top) with feedforward and (bottom) with feedback.

When all of twelve cavities are controlled by the new LLRF control system, the beam loading seen by the feedback can be different from that of the single cavity test. We performed the commissioning of the feedback starting from 500 kW equivalent beam. All of eight feedbacks could be closed up to 620 kW equivalent, however, at higher intensities some compromises had to be made to prevent rf trips. Namely, the harmonic feedback should be turned off for problematic cavities, starting with ($h = 8$), and if this did not solve the problem, the voltage pattern should be lowered.

To realize stable acceleration of 1 MW equivalent beam, it was necessary that (1) compensation up to ($h = 6$) for five and ($h = 5$) for seven of the twelve cavities, and (2) for one cavity, a voltage pattern with a factor of 0.9. The harmonic components of the vector sum voltage of twelve cavities with the conditions above are plotted in the top of Fig. 3. The driving harmonics ($h = 2, 4$) are regulated as programmed. The amplitudes of up to 40 kV and 25 kV are observed for the (partially or fully) uncompensated harmonics ($h = 6, 8$), compared to a maximum voltage of 440 kV for the accelerating frequency ($h = 2$).

Although a compromise in the feedback setting had to be made, very stable beam acceleration of 1 MW equivalent beams is realized. The mountain plot of the beam signal from injection to extraction is shown in the middle of Fig. 3. One can see that the acceleration is stable without longitudinal oscillations or instabilities. The harmonic components of the beam signal are plotted in the bottom of Fig. 3. The amplitude of the harmonic components of the beam signal change smoothly without oscillation, indicating that the bunch shape changes slowly during acceleration.

The beam acceleration with the feedback is more stable than that with the feedforward in the original system. For the cases of the feedforward and feedback, the momentum

Content from this work may be used under the terms of the CC-BY-4.0 licence (© 2023). Any distribution of this work must maintain attribution to the author(s), title of the work, publisher, and DOI

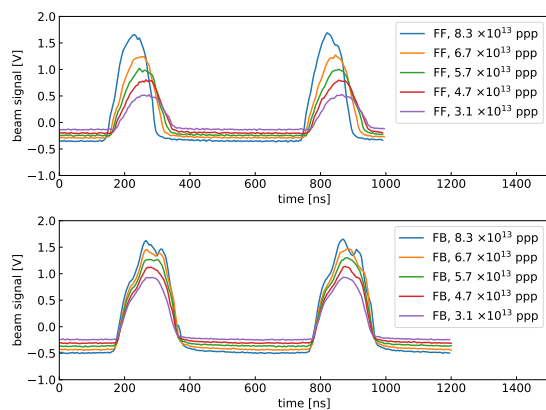


Figure 5: Beam signals just before extraction for various beam intensities, (top) with feedforward and (bottom) with feedback.

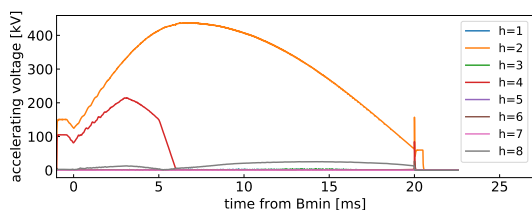
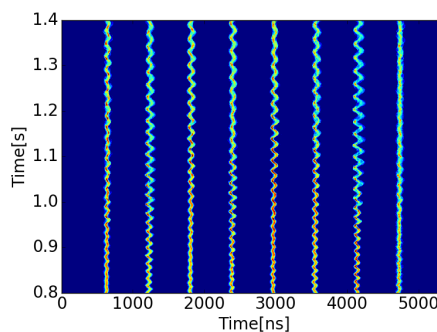


Figure 6: Harmonic components of the cavity voltage vectorsum with compensation up to ($h = 6$) for all cavities.

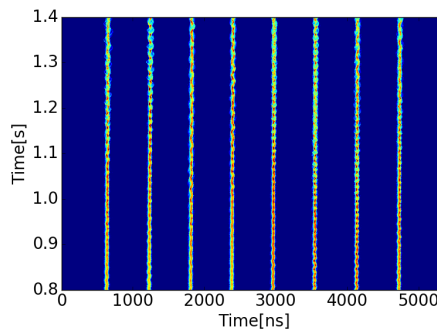
deviations (dp/p) from injection to extraction with various intensities are plotted in Fig. 4. In both cases, there is no intensity dependence of dp/p up to 10 ms. In the case of the feedforward, there is a small dependence from 10 ms to 17.5 ms, followed by a strong intensity dependence near extraction. The programmed voltage is reduced down to 60 kV near extraction and the effect of the remaining wake voltage due to the imperfection of compensation becomes large. The maximum deviation is large as 0.1%. In case of the feedback, the dependency is small, within 0.01%.

The intensity dependence of the bunch shape just before extraction is shown in Fig.5. In case of the feedforward, the timing changes by about 40 ns depending on the intensity. This is considered to be due to the rf phase change because of imperfection of the beam loading compensation. The intensity dependence of bunch timing is very small in case of the feedback.

The compromise in the feedback setting described above comes from the increase of the distortion of the amplifier chain at very high output close to its limit. Consolidation of the amplifier chain seems to be essentially necessary. Also, it is also useful to re-adjust the parameters of the tetrode in the final stage amplifier. The tetrode (TH589) has been operated with the filament current of 450 A in order to extend tube life. By increasing the filament current to 480 A and the screen grid voltage from 1.75 kV to 2.0 kV, the gain of the final stage amplifier can be increased and the load on the drive stage amplifier can be reduced. With the operating



(a) With feedforward.



(b) With feedback.

Figure 7: Mountain plots of the beam signals of 475 kW beams.

condition, the ($h = 6$) feedback loops for all cavities can be closed, while the ($h = 8$) feedback loops are still disabled. The harmonic components of the cavity voltage vectorsum with compensation up to ($h = 6$) for all cavities are plotted in Fig. 6. Compared to Fig. 3, one can see that the ($h = 6$) component is well suppressed.

These results indicate that it is necessary to consider the high power rf system as well as the LLRF control for realizing high intensity beam acceleration.

MR Beam Commissioning Results

In the MR, the longitudinal coupled bunch instability has been observed above the beam power of 450 kW and a limiting factor of the available beam power. The wake voltages of the neighbor harmonic ($h = 8, 10$) were considered to be the source of oscillations based on the mode analysis. The multiharmonic feedforward could reduce the neighbor harmonic components by a factor, however, the reduction was not enough.

The multiharmonic feedback could significantly reduced the neighbor harmonic components. The mountain plots of the beam signals at 475 kW are compared in Fig. 7. One can see that the oscillation is suppressed with the multiharmonic feedback. The user beam operation at 510 kW for the neutrino experiment has been achieved.

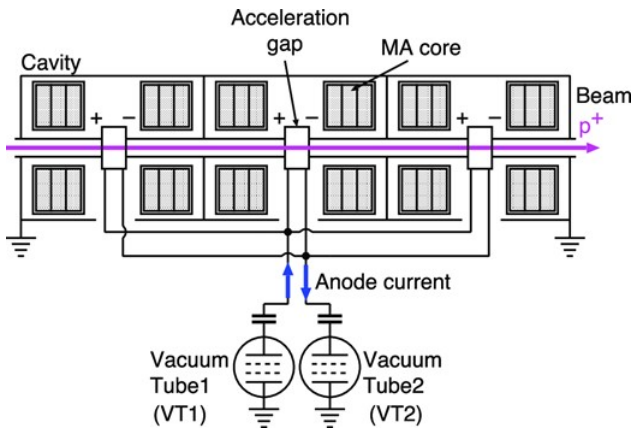


Figure 8: Simplified schematic diagram of the RCS cavity.

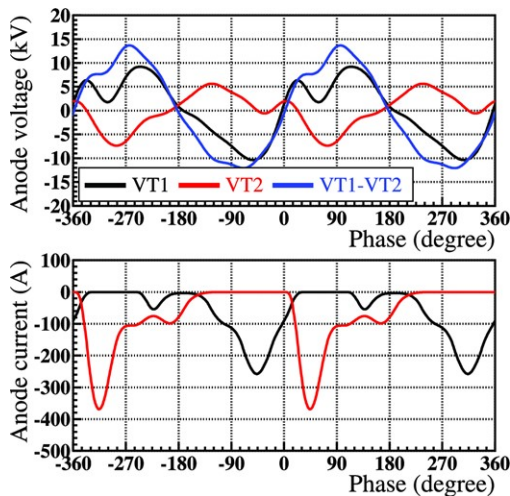


Figure 9: Simulated anode voltages and currents for the 1 MW beam acceleration in the push-pull operation.

SINGLE-ENDED CAVITY FOR RCS

Analysis of the Tetrode Operating Conditions

As described in the previous section, rf trips may occur in some conditions when high intensity beam is accelerated. To investigate the tetrode operating condition, a comprehensive simulations have been performed [15]. For the simulations, the tetrode model and the complete impedance model including the cavity, busbars, inductors, capacitors and the other rf components are developed. The beam loading compensation is also considered. A simplified schematic diagram of the RCS cavity is illustrated in Fig. 8. The cavity is driven by the push-pull configuration, the VT1 and VT2 are connected to the upstream and downstream gaps. This configuration is employed so that the distortion due to the second harmonic is cancelled.

By the extensive simulations, we found that the combination of the wideband rf cavity and the push-pull amplifier may cause serious imbalance of the operating condition of VT1 and VT2. The simulated anode voltages and currents of the VT1 and VT2 when 1 MW equivalent beam is accelerated are plotted in Fig. 9. The anode voltages and currents

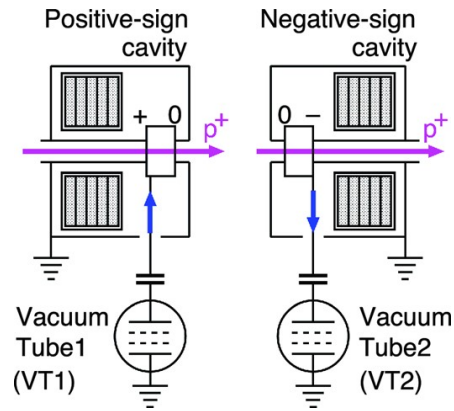


Figure 10: Positive-sign and negative-sign cavities for simulation.

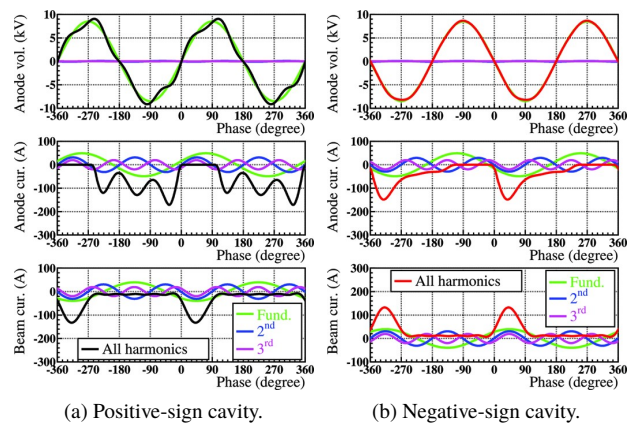


Figure 11: Simulated anode voltages, currents, and beam currents for the 1 MW beam acceleration in the single-ended operation. The harmonic components of the currents are also plotted.

are not symmetric on both tetrodes. Furthermore, the large imbalance of the anode voltage appears and the amplitude of VT1 is quite larger than that of VT2. The large amplitude anode swing may cause the increase in the screen grid current. The anode voltage should not be below the screen grid voltage; the simulation shows that the current 1 MW beam operation is close to the operation limit of the tetrode.

To investigate the source of the imbalance on the tetrodes in the push-pull operation with the multiharmonic rf driving, we consider two types of a single-ended cavity [16] as shown in Fig. 10. The positive-sign cavity generates a positive voltage during the beam passage and a negative-sign cavity vice versa.

The simulated anode voltages, currents, and beam currents for the 1 MW beam acceleration in the single-ended operation are plotted in Fig. 11. The harmonic components of the currents are also plotted in the figure. In the simulation, the beam loading is compensated up to third harmonic.

The simulated anode currents of (a) positive-sign and (b) negative-sign are quite different. The anode DC current fed to the anode can be obtained by integrating the current wave-

Content from this work may be used under the terms of the CC-BY-4.0 licence (© 2023). Any distribution of this work must maintain attribution to the author(s), title of the work, publisher, and DOI

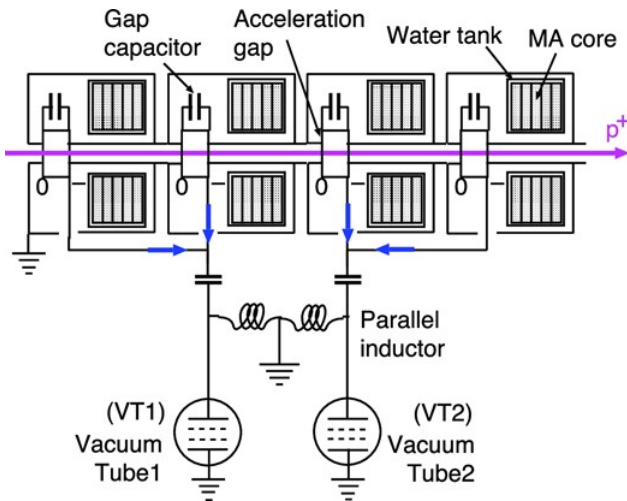


Figure 12: Simplified schematic diagram of the new single-ended cavity.

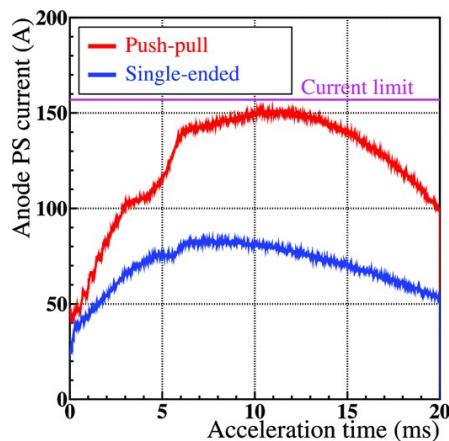


Figure 13: Comparison of the anode power supply currents between the single-ended and push-pull cavities in 1 MW beam acceleration.

form. The positive-sign cavity requires much more current than the negative-sign cavity. The complete details are described in the previous article [16] and we note here only the conclusion. The second harmonic component is the origin of the imbalance between positive-sign and negative-sign cavities. The same condition should occur in the push-pull operation because it is a combination of the positive-sign and negative-sign cavities. The second harmonic induces the severe imbalance of the anode voltage and current in the push-pull operation.

Implementation and Tests of Single-ended Cavity

According to the simulation results, we developed a new single-ended cavity, which consists of four negative-sign accelerating gaps. A simplified schematic view of the new single-ended cavity is illustrated in Fig. 12. One tetrode is connected to two acceleration gaps by the busbar and the other tube is also connected to the remaining two acceleration gaps. The tetrodes are operated in-phase, contrary to

the push-pull operation. The length of the cavity is the same as the original cavity (1950 mm). The total number of the MA core is increased from 18 (original) to 20 (single-ended). The MA core type is changed from FT3M to FT3L [17], so that a higher shunt impedance is realized. The maximum rf voltage of the single-ended cavity is the same as the original cavity, 36 kV.

The prototype cavity was constructed and an offline high-power test was performed for 1000 hours. The result was successful, no cavity impedance change was observed. One of the RCS cavity was replaced with the prototype cavity and beam acceleration of high intensity beams up to 1 MW was successfully demonstrated.

The anode power supply currents of the single-ended and push-pull cavities in 1 MW beam acceleration are compared in Fig. 13. In case of the push-pull cavity, the maximum current reaches 150 A, which is close to the power supply limit. The current is much reduced in case of the single-ended cavity and enough margin is secured. The average power is reduced from 820 kW (push-pull) to 487 kW (single-ended), thus, 40% reduction is achieved.

The prototype single-ended cavity is now operated for the user beam operation without problems.

CONCLUSION AND OUTLOOK

The application of MA cores to the accelerating rf cavities in high intensity proton synchrotrons was pioneered for the J-PARC synchrotrons. The wideband frequency response of the MA cavity has advantages and disadvantages. The new LLRF control system of the RCS and MR with the multiharmonic vector rf voltage control feedback successfully improved the multiharmonic beam loading compensation. With the new system, the stable acceleration of 1 MW is achieved in the RCS and the coupled bunch instability in the MR is suppressed.

The imbalance operation of the tetrodes in the push-pull amplifier in the RCS is essentially solved by the single-ended cavity. Furthermore, the power consumption can be greatly reduced. It is expected that 2 MW beam can be accelerated with the single-ended cavity in view of the tetrode operation [16]. We note here that the multiharmonic feedback is necessary to regulate the rf voltage of the single-ended cavity, which naturally generates more distortion due to tetrode than push-pull one.

The replacement of the RCS cavities with the single-ended cavities are in progress. Two cavities were replaced in the summer maintenance period in this year. After completion of the replacement, we will be ready to increase the beam power. The studies for the scenario beyond 1 MW beam operation are ongoing [18].

The upgrade project of the MR main magnets power supplies for shortening the cycle has been completed. The MR output beam power of 750 kW for the neutrino experiment is foreseen. The MA cavity and the new LLRF control system are expected to contribute.

REFERENCES

- [1] “Accelerator technical design report for J-PARC”, KEK, Japan, Tech. Report JAERITECH 2003-044, 2003.
- [2] K. Yamamoto *et al.*, “Design and actual performance of JPARC 3 GeV rapid cycling synchrotron for high-intensity operation,” *J. Nucl. Sci. Technol.*, vol. 59, no. 9, pp. 1174–1205, 2022. doi:10.1080/00223131.2022.2038301
- [3] T. Koseki *et al.*, “Beam commissioning and operation of the J-PARC main ring synchrotron,” *Prog. Theor. Exp. Phys.*, vol. 2012, no. 1, 2012. doi:10.1093/ptep/pts071
- [4] A. Schnase *et al.*, “MA Cavities for J-PARC with Controlled Q-value by External Inductor”, in *Proc. PAC’07*, Albuquerque, NM, USA, Jun. 2007, paper WEPMN040, pp. 2131–2133.
- [5] F. Tamura, A. Schnase, and M. Yoshii, “Dual-harmonic auto voltage control for the rapid cycling synchrotron of the Japan Proton Accelerator Research Complex,” *Phys. Rev. Spec. Top. Accel Beams*, vol. 11, no. 7, p. 072001, 2008. doi:10.1103/PhysRevSTAB.11.072001
- [6] F. Tamura *et al.*, “Longitudinal painting with large amplitude second harmonic rf voltages in the rapid cycling synchrotron of the Japan Proton Accelerator Research Complex,” *Phys. Rev. Spec. Top. Accel Beams*, vol. 12, no. 4, p. 041001, 2009. doi:10.1103/PhysRevSTAB.12.041001
- [7] H. Hotchi *et al.*, “Achievement of a low-loss 1-MW beam operation in the 3-GeV rapid cycling synchrotron of the Japan Proton Accelerator Research Complex,” *Phys. Rev. Accel. Beams*, vol. 20, p. 060402, 2017. doi:10.1103/PhysRevAccelBeams.20.060402
- [8] F. Tamura *et al.*, “Multiharmonic rf feedforward system for beam loading compensation in wide-band cavities of a rapid cycling synchrotron,” *Phys. Rev. Spec. Top. Accel Beams*, vol. 14, p. 051004, 2011. doi:10.1103/PhysRevSTAB.14.051004
- [9] F. Tamura *et al.*, “High intensity single bunch operation with heavy periodic transient beam loading in wide band rf cavities,” *Phys. Rev. Spec. Top. Accel Beams*, vol. 18, p. 091004, 2015. doi:10.1103/PhysRevSTAB.18.091004
- [10] F. Tamura *et al.*, “Multiharmonic rf feedforward system for compensation of beam loading and periodic transient effects in magnetic-alloy cavities of a proton synchrotron,” *Phys. Rev. Spec. Top. Accel Beams*, vol. 16, p. 051002, 2013. doi:10.1103/PhysRevSTAB.16.051002
- [11] F. Tamura, Y. Sugiyama, M. Yoshii, and M. Ryoshi, “Development of next-generation LLRF control system for J-PARC rapid cycling synchrotron,” *IEEE Trans. Nucl. Sci.*, vol. 66, no. 7, pp. 1242–1248, 2019. doi:10.1109/TNS.2019.2899358
- [12] PICMG, MicroTCA, <https://www.picmg.org/openstandards/microtca/>
- [13] F. Tamura *et al.*, “Multiharmonic vector rf voltage control for wideband cavities driven by vacuum tube amplifiers in a rapid cycling synchrotron,” *Phys. Rev. Accel. Beams*, vol. 22, p. 092001, 2019. doi:10.1103/PhysRevAccelBeams.22.092001
- [14] F. Tamura *et al.*, “Commissioning of the next-generation llrf control system for the rapid cycling synchrotron of the japan proton accelerator research complex,” *Nucl. Instrum. Methods Phys. Res., Sect. A*, vol. 999, p. 165211, 2021. doi:10.1016/j.nima.2021.165211
- [15] M. Yamamoto *et al.*, “Vacuum tube operation analysis under multi-harmonic driving and heavy beam loading effect in J-PARC RCS,” *Nucl. Instrum. Methods Phys. Res., Sect. A*, vol. 835, pp. 119–135, 2016. doi:10.1016/j.nima.2016.08.028
- [16] M. Yamamoto *et al.*, “Development of a single-ended magnetic alloy loaded cavity in the Japan Proton Accelerator Research Complex rapid cycling synchrotron,” *Prog. Theor. Exp. Phys.*, vol. 2023, no. 7, p. 073G01, 2023. doi:10.1093/ptep/ptad085
- [17] C. Ohmori *et al.*, “Development of a high gradient rf system using a nanocrystalline soft magnetic alloy,” *Phys. Rev. Spec. Top. Accel Beams*, vol. 16, p. 112002, 2013. doi:10.1103/PhysRevSTAB.16.112002
- [18] K. Yamamoto *et al.*, “Beyond 1 MW scenario in J-PARC rapid cycling synchrotron,” presented at HB’23, Geneva, Switzerland, Oct. 2023. paper WEC3C1, these proceedings.